Multidisciplinary mission and system design tool for a reusable electric propulsion space tug

Multidisciplinary Mission and System Design Tool for a Reusable Electric Propulsion Space Tug

Jasmine Rimani [a], Christopher Andrea Paissoni [a], Nicole Viola [a], Giorgio Saccoccia[1] , Jose Gonzalez del Amo[1]

[a] Politecnico di Torino
Department of Mechanical and Aerospace Engineering
Corso Duca degli Abruzzi, 10129, Torino, Italy
jasmine.rimani@polito.it
christopher.paissoni@polito.it
nicole.viola@polito.it

[1] European Space Research and Technology Centre (ESTEC)
Keplerlaan 1, 2201 Noordwijk AZ, The Netherlands
Electric Propulsion Section
giorgio.saccoccia@esa.int
jose.gonzalez.del.amo@esa.int

Abstract: According to the Global Exploration Roadmap, a Getaway in the lunar vicinity will enable the human exploration of the Moon, paving the way toward Mars and further in the deep space. A reusable transportation system, the Lunar Space Tug (LST), can be a key support transportation system to achieve a continuous and sustainable connection between the Earth and the orbital lunar outpost. Exploiting an electrical propulsion technology consisting in Hall Thrusters (HTs), this reusable space cargo system can maximize the delivered payload, with a lower propellant consumption with respect to a chemical-based platform. This significant improvement comes with two main throwbacks: a long transfer time between Earth and Moon and a complex multidisciplinary design of the overall LST. The first issue can be overcome with good mission planning in order to reduce the layover times and maximize the use of the LST. However, the peculiarities of the adopted propulsion technology shape the overall mass and power distribution of the space tug, as well as its transfer trajectory. The design complexity introduced by this subsystem can be effectively investigated if the mission analysis, trajectory generation and subsystem sizing are merged together in one software. In fact, the low-thrust transfer trajectories are highly affected by orbital perturbation and eclipse periods. At the same time, the high demand in power of the propulsion system puts constraints on the mass breakdown and power allocations of the LST, therefore on the reachable thrust level. The trajectory and subsystems sizing limitations call for a particular accurate mission analysis in order to succeed. Only combining all those elements, it is possible to define feasible design boundaries without performing countless simulations trying to optimize each element as a stand-alone part.

Politecnico di Torino, in collaboration with the European Space Research and Technology Centre (ESTEC), developed a MatLab-based preliminary design tool for electric propulsion space tug missions, called MultidisciplinAry desiGN Electric Tug tOol (MAGNETO). Starting from the mission analysis of the lunar space tug, the tool building blocks and capabilities are presented. Moreover, the build-in trajectory module will be analysed in-depth. The potentiality of the trajectory generation tool in MAGNETO enables a refined design of the initial design envelope of the LST. For this reason, the improved results will be confronted with the previous LST design tool developed by Politecnico di Torino.

Keywords: System Design Tool, Electric Propulsion, Reusable Space Tug, Trajectory Design

LIST OF ABBREVIATIONS

AOCS	Attitude and Orbit Control Subsystem
ConOps	Concept of Operation
e-PROP	Electric Propulsion Subsystem
EPS	Electric Power Subsystem
GEO	Geostationary Earth Orbit
GTO	Geo Transfer Orbit
HTs	Hall Thrusters
ISECG	International Space Exploration Coordination Group
LEO	Low Earth Orbit
LOP-G	Lunar Orbital Platform – Gateway
LST	Lunar Space Tug
MAGNETO	Multidisciplinary Design Electric Tug Tool
MISS	Mission and Space Systems
NRHO	Near Rectilinear Halo Orbit
TCS	Thermal Control Subsystem
TTC	Telemetry Tracking and Control

1. INTRODUCTION

The Global Exploration Roadmap [1] reaffirms the interest of the fourteen space agencies in the International Space Exploration Coordination Group (ISECG) to study and to improve critical technologies needed to enable deep space exploration. In this framework, one of the most ambitious proposed projects is the Lunar Orbital Platform-Gateway (LOP-G). Located in the cislunar space, the station may be the first human outpost above the low Earth orbit (LEO). It will be exploited as a test bench for new technologies, a scientific hub, an in-space control centre and a storage for lunar in-situ resources. To sustain the complex operations of the LOP-G, a reusable cargo spacecraft is envisioned: the Lunar Space Tug (LST). Its main goal is to reduce the operational cost while delivering cargo to and from the orbital station sustaining the habitability of the modules [2].
With the focus on maximizing the deliverable payload while keeping the transfer required propellant mass low, the adoption of the solar electric propulsion technology is one of the envisioned possibilities [2]. Because of its higher specific impulse, this technology uses a diminished amount of propellant to transfer cargo from Earth to the Moon with respect to a chemical-based spacecraft. However, this gain in mass is accompanied with longer transfer times due to the low level of thrust and high-power demand which is translated in a considerable size of the solar panels. Furthermore, the main subsystems sizing of an electric propulsion platform is highly intertwined with the transfer trajectory of the vehicle and, thus, to the thrust control strategy selected. Usually, the available tools concerning the analysis of space systems based on electric propulsion focus on the trajectory optimization given a fixed initial mass, number of thrusters and propellant (e.g. [3], [4]), or on an in-depth analysis of the propulsion system, (e.g. [5]).

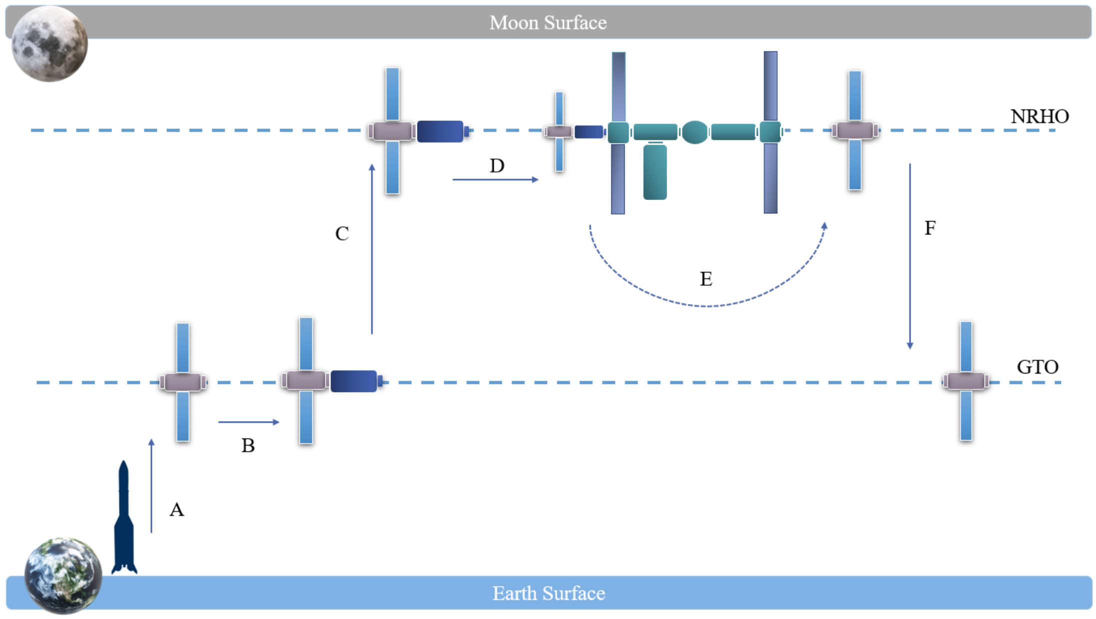

Figure 1: Design Reference Mission.

During the conceptual design phase of a space mission where diverse architectures are compared the focus lays in the identification of a feasible design envelope instead of finding an optimal solution in terms of mass or transfer time or power. Meanwhile, if those analyses can be performed maintaining low the computational time, they will ease the work of the mission analysis engineers. It is required to perform simulations with different types of propellant, thruster's operative points, number of thrusters as well as payload mass. The complexity of the problem calls for an integrated tool that may size the systems and the trajectory simultaneously at the very first phases of the design.

To answer these needs a flexible design tool is now under development by Politecnico di Torino, in collaboration with the European Space Research and Technology Centre (ESTEC). The multidisciplinary integrated tool, called "MultidisciplinAry desiGN Electric Tug tOol" (MAGNETO) performs a preliminary design of the LST in terms of main mission and system budgets. The development began with the subsystems sizing as described in ref. [6] and ended in an improved version of the masses and power definitions as well as the harmonization of a preliminary low-thrust trajectory propagation module. Moreover, MAGNETO is a flexible software that may be used to analyse different transfers and mission scenarios ranging from LEO up to lunar orbit. The in-loop trajectory tool improves the sizing results of MAGNETO in respect to the MISS software [7], another mission analysis tool of Politecnico di Torino, thanks to more accurate values of delta-V, transfer time and propellant mass.

In this paper, the case study is represented by a replenishment scenario in support to the LOP-G operation which consists of a cargo transfer from Geostationary Transfer Orbit (GTO) to Near Rectilinear Halo Orbit (NRHO). This transfer is performed exploiting the LST in which a high-power electric propulsion subsystem based on Hall Thruster (HT) is adopted. In Figure 1 is reported the design reference mission: (A) launch of the space tug, (B) docking of the LST with the Cargo, (C) orbit raising towards NRHO, (D) LST docking to the LOP-G, (D) LST undocking from the LOP-G, (E) phasing manoeuvre to avoid collision with the LOP-G, (F) de-orbiting towards the LST parking orbit.

After this brief introduction, the following section will give an overview of the tool and the mission. Then, the in-depth analysis of the trajectory modelling will be presented in Section 3. In Section 4, the results obtained will be analysed and compared with the previous data presented in [8]. After that, the last section, Section 5, will be dedicated to the main conclusions and future work.

2. TOOL STRUCTURE

Before introducing the general structure of MAGNETO and dig deeper in the trajectory generation, some details on the reference mission analysed in this paper are needed.

The functional analysis and concepts of operations are tasks performed offline with respect to the software and more details can be found in [2] and [9]. This offline analysis is performed for all the scenarios implemented in MAGNETO. As briefly introduced in the previous section, the reference mission consists in a transfer from a GTO up to NRHO ferrying a cargo payload with resupply purposes for the LOP-G.

From an operational point of view, the mission begins with the launch and initial platform commissioning operations. The LST will wait in its parking orbit until the launch of the cargo module to be transferred. The user might choose between a LEO parking orbit, a geostationary Earth orbit (GEO) parking orbit or a GTO parking orbit (as in our examined example). The different parking orbits will impose a take-off mass limitation on the LST wet mass due to the maximum launch capability of the now-conventional launchers. It is important to highlight that the LST is considered to be launched without the cargo module. The launchable mass constraint is inserted in MAGNETO and it defines if the LST configuration is feasible or not. In the case of a GTO parking orbit scenario, if the wet mass of the overall space tug is lower than 17 tons [10], the scenario may be considered reasonable in terms of launcher deliverable mass.

At the parking orbit, the LST will dock with the cargo module and will start the orbit raising towards NRHO, where the LOP-G is located. Reaching the final orbit, the LST will rendezvous with the orbiting station and the cargo handling operations will start. At the end of those operations, the LST will undock from the station and begins its return transfer towards the initial parking orbit. Reached its final destination the LST will wait for the following cargo module launch performing meanwhile the necessary on-orbit refuelling operations.

To define the requirements necessary for the design of the LST, both cargo mass and module mass are estimated considering the crewmember number, their mission duration with its incremental values taking into account the future development of the LOP-G (30, 60, 90 or 180 days of crew permanence [7]) and the number of missions per year. The daily consumables demand for each crewmember is defined in [8] and reported in equation (1). This estimation is assumed according to the requirement of the ISS and is set to 12.37 kg per person [8]. In this study, the focus is on the 60 days cargo replenishment scenario.

$$m_{cargo} = N_{crew\ member} \cdot \Delta t_{mission} \cdot N_{mission} \cdot m_{daily\ per\ member} \tag{1}$$

In general, the user may define another payload weight, or weights if different configurations are analysed. The other required data are the type of propellant, the initial orbit details and the desired final orbital parameters. Those data are inserted in an Excel file to provide a simplified user interface. During the first design iteration, the software uses its pre-loaded mass estimation budgets [2] (see **Table 1**), in order to find a first overall spacecraft mass to use during the first trajectory simulation. Moreover, the sizing routine needs to know which kind of solar panels the user wants to adopt during the simulations (e.g. Arsenio-Gallium solar cells) in order to properly size the electric power subsystem and fulfil the requirement on the power budget driven by the operations of the electric propulsion subsystem. All the design and performance characteristics of the most common solar cells can be found in the input file, but the user may modify them.

Instead, the electric propulsion operative points are stored in a different excel in terms of thrust level, specific impulse (Isp), thruster power, thruster mass and lifetime. The tool will iterative simulate the defined scenario up to LST wet mass convergence for each operative point selected in the thrusters' database. In the case study of this paper, the tool uploads the operative points of Hall Thrusters at 20 kW developed by SITAEL. **Figure**

3 shows the performance map of the selected thrusters. During this study, the focus was on the working points highlighted in the blue box defined from the mission requirement presented in [11].
In the "scenario definition" of MAGNETO is possible to define different types of electric propulsion thruster that the user wants to simulate, **Figure 2**. The tool iterates on the different working points stored in "Thruster Data". Therefore, as long as the thrust level, specific impulse (Isp), thruster power, thruster mass and lifetime are known, the type of propulsion can be changed. The tool relays on its strong modularity to analyse different types of electric propulsion missions.
In the inputs section, the type of orbit control strategy shall be defined in terms of which classical orbital parameters will be controlled during the orbit propagation and if the eclipse periods during the transfer are or not considered. The orbit control parameters shall be tailored with respect to the orbit propagation itself. For instance, if the analysis is focusing on a rendezvous manoeuvre, controlling the argument of perigee and right ascension of ascending node maybe necessary [11]. However, for a simple transfer from an orbit to another, the user may want to control only the semimajor-axis, the eccentricity and the inclination of the orbit. Inside the tool there are some suggestion on how to set the controls for different analysis.
For some more advanced trajectories, there is the possibility to indicate if the thrusters fire only when an overall efficiency in the orbital parameters' variation can be achieved or if continuously firing is enforced. In addition, the tool implements the possibility of using a thrust control law similar to the one adopted for SMART-1 [12], that resulted very efficient in terms of propellant mass management [13]. The key point of SMART-1 propellant saving was due to the thrusting laws: most of the thrusting was concentrated in the proximity of perigee for most part of the trajectory [13], just above the Van Allen belts and almost up the lunar orbit.
The in-loop trajectory analysis is extensively investigated in Section 3. The tool implements a suboptimal trajectory propagation process: at each step of the simulation, the local optimum is evaluated knowing the set control and the final desired orbital position. This approach enables a fast computation of the overall trajectory, thus making it suitable for a closed loop conceptual design tool.
After the definition of the simulation parameters, the focus shifts toward the scenario analysis, **Figure 2**. The final preliminary sizing of the subsystems is highly dependent of the trajectory analysis. At the same time the trajectory will be highly affected by the mass and available power.

Table 1 : The Lunar Space Tug Mass Breakdown

Subsystem	Relative Percentage [%]	Safety Margin [%]
AOCS	9	-
e-PROP	24	-
EPS	36	-
TCS	13	-
TTC	1	20
CDH	1	20
Structure and Mechanism	16	10

Inside MAGNETO, there is a dedicated module to size the main space tug subsystems in terms of mass and power. The sizing focuses on the in-depth analysis of four main subsystems: (i) Attitude and Orbit Control Subsystem (AOCS), (ii) Electric Propulsion Subsystem (e-PROP), (iii) Electric Power Subsystem (EPS), (iv) Thermal Control Subsystem (TCS). The other considered subsystems are (v) Structure and Mechanism, (vi) Control and Data Handling (CDH), (ii) Telemetry Tracking and Command (TTC). The mass of the latter set of subsystems is evaluated as a percentage of the total spacecraft dry mass reported in **Table 1** during the overall simulation. During the first iteration of the tool all the subsystems' masses are computed following the mass breakdown in **Table 1**, and all the safety margins set at 20% if not otherwise specified. Then, from the second iteration, the sizing of the first four subsystems is addressed in detail following the formulations in ref. [6] and

extensively analysed in detail in ref. [9]. Therefore, for these first subsystem the safety margins are taken at component level. Hence, no other safety margin at subsystem level on the final resulting mass and power. All the safety margins included at subsystem or component level are derived from the ESA safety margin philosophy in ref. [14].
Overall, the values reported in **Table 1** are based on an extensive study conducted by PoliTO on the sizing of an unmanned space tug and documented in [2], [7] , [8], [9]. The study merged the different concepts of envisioned space tugs with the sizing rules for satellites exploiting electric propulsion and ISS cargo modules. All the information is stored in a database that can be extended to refine the estimation of the mass and power breakdowns of a reusable space tug. This are high-level assumption that will be refined in the subsystem sizing module of MAGNETO. **Figure 1**
However, the input mass breakdown can affect the overall estimation of the dry mass, therefore, the wet mass and the trajectory. This is especially noticeable for the subsystems defined only by relative percentage in **Table 1**. Due to this interdependence of overall sizing and trajectory computation, it is possible to change the initial mass breakdown and the considered margins in the input file related to the "scenario definition" in **Figure 2Figure 1**.

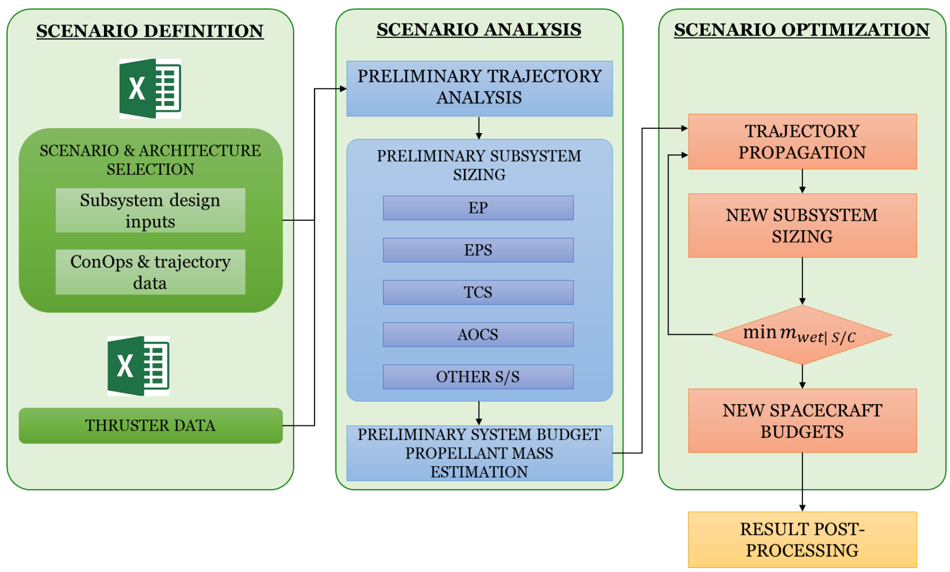

Figure 2: High-level MAGNETO structure and building blocks

Following the scenario analysis and preliminary system sizing, the tool performs the optimization of the initial design solutions: it iterates between the trajectory section and the sizing section until a convergence of the masses is reached. The objective of the tool is the minimization of the wet mass, while computing the overall trajectory.
MAGNETO is intended and built to be modular: it is easy to add functionalities or modify and enhance the design of subsystem or the mathematical definition of the trajectory perturbations. Moreover, it is possible to use the trajectory tool as a standalone software as well as the subsystem design part.

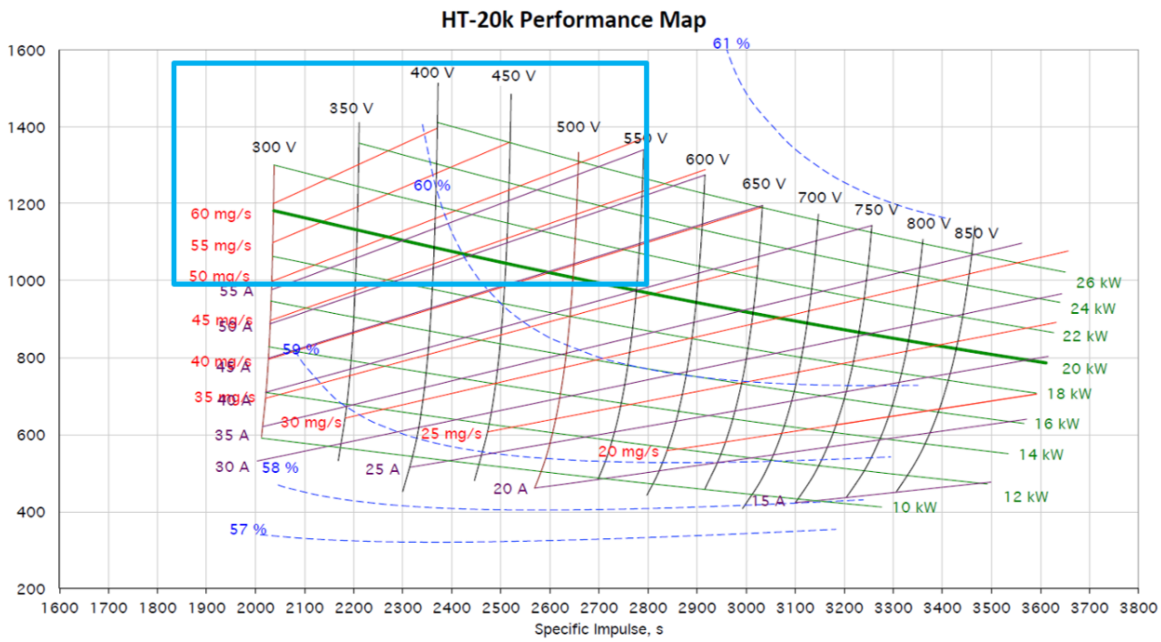

Figure 3: Hall Effect Thrusters Functional Map (credits: SITAEL). The data range used in the simulation is highlighted in the blue box. the points in the database are specified by the intersections between the power (kW) and the voltage (V).

3. TRAJECTORY ANALYSIS

The core of MAGNETO is the in-loop trajectory generation tool: a fast and reliable computation of the propellant mass, transfer time and delta-V inside a sizing routine. The previous PoliTO mission analysis software, MISS, relayed on a simplified formulation of the delta-V [8], in the framework of Endelbaum approximations for low-thrust manoeuvres [4]. The transfer time was based on an analytical fitting of the data presented in ref. [13], related to standard "LEO to GEO" transfers and typical low-thrust lunar trajectories, with results compliant with SMART-1 trajectory. The propellant mass was evaluated with Tsiolkovsky rocket equation [6]. The limits of this approach lay in the incapacity of simulating diverse scenarios, where different orbits or control strategies are of interest. Although, the use of simplified formulations optimizes the computational time of the closed loop software: MAGNETO, had the main requirement of enabling a better accuracy keeping the computational time low. Those refined data will be the inputs that will enable a more accurate evaluation in the system sizing routine.

The trajectory have been validated with the literature values in ref. [13] and using commercial software like GMAT (General Mission Analysis Tool) and STK (System Tool Kit), **Table 2**.

Table 2: Tool Validation results, LEO to GEO trajectory end values. The total mass is 7 tons, with 6 N of thrust and 2800 s of Isp.

Parameter	GMAT	MAGNETO	% DIFFERENCE
Semi-major axis [km]	4.2166e+04	4.2167e+04	0.003%
Eccentricity	0.0083	0.0076	1%
Orbital Inclination [deg]	0.9688	1.0275	1%
Time [days]	59.4	59.3	0.005%
Propellant Mass [kg]	1052	1048	0.004%

Delta V [km/s]	4.47	4.5	0.7%

In MAGNETO, the overall spacecraft orbital dynamics is modelled using a set of modified equinoctial elements exploiting a patched conics approximation. This approach was considered sufficiently accurate for the preliminary trajectory analysis performed by the design tool, seen the good comparison with the results of GMAT and literature data in ref. [13].
The software implements the zonal harmonics gravity model up to J2-gravity perturbation. Moreover, preliminary models of solar pressure and atmospheric drag are introduced. The main approximation considered for the latter two perturbation is the constant exposed surfaces during all the simulation. Furthermore, the three-body perturbations of Sun and Moon are considered during the transfer in the Earth sphere of influence. Likewise, the Sun and Earth perturbations are considered in the Cislunar space. All those disturbances can reach magnitudes equivalent to the thrust acceleration, e.g. the solar radiation pressure acting on broad solar panels, therefore they must be included within the analysis. Moreover, the thrusters are operated only during the sunlight period of the orbit. Based on the overall mass of the vehicle, the eclipse can heavily shape the trajectory due to the other perturbations.
In the tool, the level of thrust is considered constant during all the transfer phases and depends on the analysed operative point. Instead, the resultant thrust acceleration varies with the variation of the wet mass of the spacecraft: as the mass decreases, the thrust acceleration increases. The thrust is divided in a normal, tangential and radial component along the spacecraft orbit, in the Local Vertical – Local Horizontal (LVLH) reference system. In order to reach the desired final orbital values, MAGNETO exploits a weighted method, eq. (2).

$$W_i = \frac{v_{orbital}(t) - v_{target}}{|v_{initial} - v_{target}|} \tag{2}$$

The weight, W_i, is evaluated considering an orbital parameter value at the instant t ($v_{orbital}(t)$), its target value (v_{target}) and its initial value ($v_{initial}$). The thrust function will aim to reach the final desired value of the i_{th} orbital parameter minimizing the weight W_i. At each step, the tool tries to diminish the different weights for the different controlled orbital parameters. This method generates a locally optimal trajectory, therefore, considering the repetition of the process for each integration step, a global suboptimal trajectory. The weights are considered with sign: this is an indication of the "direction" of the perturbation needed to cancel the difference between the $v_{orbital}(t)$ and the target value.
The complete mathematical model exploited in the software is reported in the following Subsection 3.1. The focus of the formulation lays in the definition of the thrust control strategy and the validation of the trajectory propagation routine.

3.1 Mathematical Model

The motion of a spacecraft can be described with a second order differential equations [15] in the cartesian reference system, equation (3). The central body may be Earth (ECI, Earth Cantered Inertial), when in the Earth space or Moon in the Cislunar Space.

$$\ddot{\boldsymbol{r}} + \mu \frac{\boldsymbol{r}}{r} = \boldsymbol{a}_p \tag{3}$$

Where (i) $r = \|\mathbf{r}\|$ is the modulus of the radius $\mathbf{r}$ of the S/C position with respect to the central body, (ii) μ is the gravitational constant referred to the central body, (iii) $\mathbf{a}_\mathrm{p}$ are the perturbing accelerations that change the spacecraft state in the ECI system.
From the cartesian definition of the equations of motion, it is possible to switch towards the modified equinoctial elements [15], for which the relation with the cartesian parameter are defined in the system of equation (4). This

switch will enable a more time effective simulation [16]. Therefore, the overall dynamics model exploited in the tool can be expressed as reported in equation (5) to equation (11).

$$
\begin{gathered}
p = a(1 - e^2) \\
f = e \cdot cos(\omega + \Omega) \\
g = e \ \cdot \sin(\omega + \Omega) \\
h = \tan(i/2) \cos\ \Omega \\
k = \tan(i/2) \sin \Omega \\
L = \Omega + \omega + \theta
\end{gathered} \tag{4}
$$

where: (i) “p” is the semi-parameter (semi-latus rectum), (ii) “a” is the semi-major axis, (iii) “e” is the orbital eccentricity, (iv) “i” is the orbital inclination, (v) “ω" is the argument of perigee, (vi) “Ω” is the right ascension of the ascending node, (vii) “θ” is the true anomaly, (viii) “L” is the true longitude.

$$\dot{y} = A(y)\Delta + b \tag{5}$$

$$y = [p, f, g, h, k, L] \tag{6}$$

$$
A(y) = \begin{bmatrix}
0 & \frac{2p}{q}\sqrt[2]{\frac{p}{\mu}} & 0 \\
\sqrt[2]{\frac{p}{\mu}} \sin L & \sqrt[2]{\frac{p}{\mu}} \frac{1}{q}\{(q+1)\cos L + f\} & -\sqrt[2]{\frac{p}{\mu}} \frac{g}{q}\{h \sin L - k \cos L\} \\
-\sqrt[2]{\frac{p}{\mu}} \cos L & \sqrt[2]{\frac{p}{\mu}} \frac{1}{q}\{(q+1)\sin L + g\} & \sqrt[2]{\frac{p}{\mu}} \frac{f}{q}\{h \sin L - k \cos L\} \\
0 & 0 & \sqrt[2]{\frac{p}{\mu}} \frac{s^2 \cos L}{2q} \\
0 & 0 & \sqrt[2]{\frac{p}{\mu}} \frac{s^2 \sin L}{2q} \\
0 & 0 & \sqrt[2]{\frac{p}{\mu}} \frac{1}{q}\ \{h \sin L - k \cos L\}
\end{bmatrix} \tag{7}
$$

$$b = \left[0\ 0\ 0\ 0\ 0\ \sqrt[2]{\mu p} \left(\frac{q}{p}\right)^2 \right] \tag{8}$$

$$
\begin{aligned}
\Delta = [\, a_{radial}\ a_{tangential}\ a_{normal}] \\
= \Delta_{oblate\ earth} + \Delta_{\text{third}\ body} + \Delta_{thrust} + \ \Delta_{drag}\ + \ \Delta_{solar\ pressure}
\end{aligned} \tag{9}
$$

$$q = 1 + f \cos L + g \sin L \tag{10}$$

$s^2 = 1 + \sqrt[2]{h^2 + k^2}$	(11)

Where the parameter "Δ" considers five perturbing accelerations expressed in the LVLH frame [17]: J2-gravity perturbation, third body perturbation, thrust acceleration, drag and solar pressure. The thrust acceleration results usually predominant during sunlight periods with respect to the others, that show their major effect during eclipse [18].

The first analysed acceleration is the J2-gravity perturbation. It is first expressed in the centred inertial reference system (equation (12) to equation (14)) and then transformed in the LVLH frame [19], equation (15). This perturbation is included during both the Earth transfer and the Cislunar space transfer, with their respective J2 values.

$g_{xj2} = -3 * \mu * J2 * \frac{r_{equatorial}^2}{2 * r^4} * \left(1 - 5 * \frac{Z}{r}\right) * \left(\frac{X}{r}\right)$	(12)
$g_{yj2} = -3 * \mu * J2 * \frac{r_{equatorial}^2}{2 * r^4} * \left(1 - 5 * \frac{Z}{r}\right) * \left(\frac{Y}{r}\right)$	(13)
$g_{zj2} = -3 * \mu * J2 * \frac{r_{equatorial}^2}{2 * r^4} * \left(3 - 5 * \frac{Z}{r}\right) * \left(\frac{Z}{r}\right)$	(14)
$\Delta_{oblate\ Earth} = Q_{LVLH} * [g_{xj2} \quad g_{yj2} \quad g_{zj2}]$	(15)

Where (i) $r_{equatorial}$ is the Earth equatorial radius, (ii) J2 is the gravity perturbation, (iii) (V) X,Y,Z are the ECI coordinate of the orbit, (iv) Q_{LVLH} is the matrix between ECI and LVLH.

Because an initial parking orbit below 2000 km of altitude, the atmospheric drag effects cannot be neglected [19], this perturbation is included during all the simulations in the Earth proximity. The effects are important in particular during the LEO to GEO transfers or LEO station-keeping operation. The drag is expressed in the ECI system and then transformed into the LVLH reference system. In the drag formula, the atmosphere relative velocity is expressed as in ref [19]. The modelling is reported from equation (16) to equation (18). The surface "A" exposed to the drag is considered as a fixed value during the simulation. It is evaluated from the shape of the LTS.

$\Delta_{drag\ ECI} = -\frac{1}{2} * C_D * \frac{A}{m} * \rho * v_{rel}^2 * \frac{\vec{v}_{rel}}{\lvert\vec{v}_{rel}\rvert}$	(16)
$\vec{v}_{rel} = \frac{\mathrm{d}\vec{r}}{\mathrm{dt}} - \vec{\omega}_{Earth}\ x\ \vec{r}$	(17)
$\Delta_{drag} = Q_{LVLH} * \Delta_{\ drag\ ECI}$	(18)

Where (i) C_D is the drag coefficient of the Tug now set to 2.2, (ii) ρ is the air density, (iii) m is the mass of the system, (iv) $\vec{v}_{rel}$ is the relative velocity of the space tug in respect to the atmosphere as defined in ref. [19], (v) $\vec{\omega}_{Earth}$ is the Earth rotation vector.

The solar pressure perturbation is expressed in the ECI system and the reported in the LVLH reference system. The solar pressure varies during the years and seasons. However, for simplification, a mean value was assumed in MAGNETO [19]. Equation (19) to and equation (20) report the formulation of this perturbation. Again, the surface “A” is considered constant through the trajectory the simulation. Updates on this model are now under development to have a more precise modelling of this perturbation and on the exposed surface.

$\Delta_{solar\ presseure\ ECI} = -\frac{p_{SR} * c_R * A}{m} * \frac{\vec{r}}{\lvert\vec{r}\rvert}$	(19)
$\Delta_{solar\ pressue} = Q_{LVLH} * \Delta_{solar\ presseure\ ECI}$	(20)

Where (i) p_{SR} is the solar pressure value as in ref [19], (ii) c_R is the reflectivity coefficient, (iii) $\vec{r}$ is the radius vector of the space tug orbit.
The third body perturbation is evaluated using Battin’s method [18], in order to avoid cancellation of the lower order terms [20]. Equations (21) to (24) show the mathematical model of the perturbation with Earth as central body. The equations used for the Moon are analogous.

$\Delta_{third\ body} = -\frac{\mu_{sun}}{\boldsymbol{d_s^3}}\left[\boldsymbol{r} + F(q_s) * \boldsymbol{s_s}\right] - \frac{\mu_{moon}}{\boldsymbol{d_m^3}}\left[\boldsymbol{r} + F(q_m) * \boldsymbol{s_m}\right]$	(21)
$F(q_s) = q_s\left[\frac{3 + 3q_s + q_s^2}{1 + \left(\sqrt{1 + q_s}\right)^3}\right] \quad q_s = \frac{\boldsymbol{r^T}(\boldsymbol{r} - 2\boldsymbol{s_s})}{\boldsymbol{s_s^T s_s}}$	(22)
$F(q_m) = q_m\left[\frac{3 + 3q_m + q_m^2}{1 + \left(\sqrt{1 + q_m}\right)^3}\right] \quad q_m = \frac{\boldsymbol{r^T}(\boldsymbol{r} - 2\boldsymbol{s_m})}{\boldsymbol{s_m^T s_m}}$	(23)
$\boldsymbol{d_s} = \boldsymbol{r} - \boldsymbol{s_s} \qquad \boldsymbol{d_m} = \boldsymbol{r} - \boldsymbol{s_m}$	(24)

Where (i) d_s is the vector between the Sun and the space tug, (ii) d_m is the vector between the Moon and the space tug, (iii) s_s is the vector between the Earth and the Sun, (iv) s_m is the vector between the Earth and the Moon, (v) μ_{sun} is the gravitational constant of the Sun, (vi) μ_{moon} is the gravitational constant of the Moon, (vii) r is the radius of the orbit.
The last perturbation analysed in the MAGNETO is the thrust acceleration. The thrust level is considered constant during all the simulation, a part of the eclipse periods where the thruster is not operated. The thrust acceleration varies with the mass of the vehicle, equation (25), that it is evaluated at each step of the simulation.

$a_{thrust} = \frac{thrust_{LST}}{mass_{LST}}$	(25)

This thrust acceleration is divided in the radial, tangential and normal direction in accordance with the weights defined in equation (2), equation (26).

$$\Delta_{\text{thrust}} = a_{thrust} * \vec{u} = a_{thrust} * \begin{bmatrix} u_{radial} \\ u_{tangetial} \\ u_{normal} \end{bmatrix}$$	(26)

More in detail, for each orbital element, the maximum needed perturbation is divided in the three reference directions of the LVLH reference system starting from the thrust angles (in-plane angle α, out-of-plane angle β) that maximize the perturbation contribution of the related orbital element. Beginning from the cartesian definition of the orbital parameters, the in-plane angle and out-of-plane angle are defined in **Table 3** [21].

Table 3: In plane and out of plane values that can maximize the different orbital parameters [21]

Orbital Parameter	In-plane angle	Out-of-plane angle
Semi-major axis a	$\alpha = \tan^{-1}\left(e \cdot \frac{\sin \nu}{1 + e \cdot \cos \nu}\right)$	$\beta = 0$
Eccentricity e	$\alpha = \tan^{-1}\left(e \cdot \frac{\sin \nu}{\cos \nu + \cos E}\right)$	$\beta = 0$
Inclination i	$\alpha = 0$	$\beta = \mathrm{sgn}\left(\cos\,(\omega + \nu)\right) \cdot \frac{\pi}{2}$
RAAN* Ω	$\alpha = 0$	$\beta = \mathrm{sgn}\left(\sin\,(\omega + \nu)\right) \cdot \frac{\pi}{2}$
Argument of Perigee ω	$\alpha = \tan^{-1}\left(\frac{1 + e \cdot \cos \nu}{2 + e \cdot \cos \nu} \cdot \cot \nu\right)$	$\beta = \tan^{-1}\left(\frac{e \cdot \cot i \sin\,(\omega + \nu))}{\sin(\alpha - \nu) \cdot (1 + e \cdot \cos \nu) - \cos \alpha \cdot \cos \nu}\right)$
*RAAN: Right Ascension of the Ascending Node ∗ ν is the true anomaly		

From each orbital parameter, the maximum perturbation derived to achieve the target value is weighted and summed to find the resultant in the radial, tangential and normal directions, equation (27) to equation (29). Those values are still not normalized: the resultants may not be unitary. Thus, the vector containing the perturbations is normalized to respect the path constraint of unitary vector (equation (30) and equation (31)).

$$u_{radial} = W_a \cdot \cos(\beta_{max_a}) \cdot \sin(\alpha_{max_a}) + W_e \cdot \cos(\beta_{max_e}) \cdot \sin(\alpha_{max_e}) + W_w \cdot \cos(\beta_{max_w}) \cdot \sin(\alpha_{max_w})$$	(27)
$$u_{tangetial} = W_a \cdot \cos(\beta_{max_a}) \cdot \cos(\alpha_{max_a}) + W_e \cdot \cos(\beta_{max_e}) \cdot \cos(\alpha_{max_e}) + W_w \cdot \cos(\beta_{max_w}) \cdot \cos\,(\alpha_{max_w})$$	(28)
$$u_{normal} = W_a \cdot \sin(\beta_{max_a}) + W_e \cdot \sin(\beta_{max_e}) + W_w \cdot \sin(\beta_{max_w}) + W_i \cdot \sin(\beta_{max_i}) + W_{RAAN} \cdot \sin(\beta_{max_{RAAN}})$$	(29)

Eventually, the vector $\vec{u}$ is a unitary vector derived from the maximum perturbation in terms of in-plane angle α and out-of-plane angle β of each controlled orbital parameter [21].

$$\overrightarrow{|u|} = 1 \tag{30}$$

$$\vec{u} = \frac{(\sum \vec{u}_{perturbation_{max}})}{|(\sum \vec{u}_{perturbation_{max}})|} \tag{31}$$

At the end of this process the overall thrust angles α and β can be computed from the components of $\vec{u}$ [20]:

$$\alpha = atan2\left(\frac{u_r}{u_t}\right) \tag{32}$$

$$\beta = \text{asin}\,(u_n) \tag{33}$$

The eclipse function is based on a spherical model assuming Earth and Sun as spherical body [22]. The JPL SPICE model [23] is exploited to acquire the information on the relative position of the Earth-Sun-Spacecraft system.

4. MAIN RESULTS AND COMPARISON WITH THE PREVIOUS OUTPUTS

As previously introduced, the main results of a scenario simulation consist in the LST subsystems' mass and power budgets, the overall dry and wet mass of the LST and the preliminary suboptimal low-thrust trajectory. In this section the results for the reference scenario of a 60 days cargo transfer mission from GTO to NRHO performed by the LST is presented. It is just one of the many possible examples of the applications of this tool. The previous results of MISS presented in ref. [8] are based on a transfer time logic similar to the SMART-1 like trajectory from [13]. To compare the outputs, the same control and thrust strategy were used. The scenario focuses on a 60-days replenishment cargo mission with four HTs. The results presented in **Table 4** and **Table 5**, refer to the resulted optimal configuration (Isp = 2100 s, Thrust = 1.05 N, Power = 18 kW, Number of Thrusters = 4) after the trade-off analysis. The trade-off was performed between the different sets of sizing and trajectory outputs for each of the working points highlighted in **Figure 3**, [8]. The figures of merit included are (i) power, (ii) dry mass, (iii) propellant mass, (iv) transfer time. The propellant mass reported considers the complete round trip which strongly impacts the sizing of the system. The mission ConOps, summarized in section 2, assumes to adopt an on-orbit refuelling system located in Earth orbit.

Table 4: Typical sizing results for a 60-days-replenishment cargo with four HTs

Cargo Mass	5.4	[tons]
Total Mass	13.6	[tons]
Dry Mass	5.9	[tons]
Propellant Mass GTO-NRHO	1.3	[tons]
Propellant Mass NRHO-GEO	0.8	[tons]
Total Power	171	[kW]
e-PROP Mass	692	[kg]
e-PROP Power	91	[kW]
AOCS Mass	300	[kg]
AOCS Power	1.6	[kW]

Solar Array Area	587	$[m^2]$
Solar Array Mass	1018	[kg]
EPS Mass	2063	[kg]
TCS Mass	750	[kg]
TCS Power	7	[kW]
CDH Mass	57	[kg]
COMM Mass	57	[kg]
Structure and Mechanism Mass	816	[kg]
Others Power	71	[kW]

The SMART-1 like trajectories are very efficient in terms of propellant mass due to their control strategy and resonant orbits. However, the patched conics approximation cannot be perfectly replicated due to the Moon resonance effects neglected in the trajectory model introduced. Considering this throwback, we defined a control strategy similar to the SMART-1 one as reported in [13]. More in detail, the SMART-1 mission control was divided in three main segments:

- Continuously thrusting to raise the perigee up to 20000 km, in between the Van Allen belts [13].
- Intermitted thrusting to raise the apogee near the perigee [13].
- Continuously thrusting adjusting the eccentricity, the semimajor axis and the inclination to reach the Moon [13].

In MAGNETO this logic is implemented: more in detail, in the second phase, the intermitted thrusting is performed only when the manoeuvre can guarantee at least 70% of efficiency in raising the apogee.
The results found with this strategy were compliant with the SMART-1 parameters in terms of delta-V and transfer duration [13]. The trajectory outputs are presented in **Table 5**, while **Figure 4** shows the trajectory generated by the tool for the considered scenario.

Table 5: Typical trajectory results for a 60-days-replenishment cargo with SMART-1 like thrust strategy

Delta-V Earth to Moon transfer	2.4	[km/s]
Transfer Time GTO-NRHO	364	[days]

The optimal configuration presented and selected in [8] will be used as a comparison mean for the new results. **Table 6** reports the comparison between MISS and MAGNETO outputs. The optimal working point for the MISS software was defined as a four thrusters' configuration with Isp of 2600 s, thrust of 1.025 N and power of 20 kW. While, the optimal working point individuated by MAGNETO is a four-thruster configuration with Isp of 2100 s, thrust of 1.05 N and power of 18 kW.

Table 6: Comparison with the previous results [8] **for the optimal design sizing for 60-days replenishment (Isp = 2100 s, Thrust =1.0500 N, Power = 18 kW)**

Parameters	MISS Results	MAGNETO (MISS v2) Results	Percentage
Propellant Mass GTO-NRHO [kg]	1976	1340	-32%
Propellant Mass NRHO-GTO [kg]	1255	771	-39%
LST Dry Mass [kg]	5241	5964 (*)	+12%
LST Wet Mass [kg]	15622	13645	-9%
Transfer Time GTO-NRHO [days]	480	364	-25%
(*) Different assumption on EPS, TCS and AOCS. The dry mass isn't comprehensive of the cargo mass.			

In compliance with the obtained results, the SMART-1 like trajectory is very efficient in terms of propellant consumption. The dry mass from MAGNETO is the 12% more of the MISS output: in the new version of the tool, the dry mass is studied more in detail and with more severe design margins, typically adopted in the preliminary conceptual mission design phase. The EPS considers a power processing unit (PPU) for each thruster, while in MISS a single PPU was connected to four thrusters through a Thruster Switching Unit (one operative thruster and the other in cold stand-by). The TCS analyses a wider temperature interval based on the maximum and minimum allowable temperature of each subsystem. The AOCS is evaluated considering the rendezvous constraints explained in [9], keeping into account the overall mass and dimension of the LST. The overall wet mass is diminished in respect to MISS thanks to a more accurate calculation of the propellant mass. This allows a 25% of difference between the MISS and MAGNETO transfer time outputs. In **Table 7**, the values of the MAGNETO design for the MISS optimal solution working point are reported and compared. Likewise, the MAGNETO estimated propellant mass is less than the one resulted from MISS. Overall, MAGNETO permits to refine the preliminary design data.

Table 7: Comparison with the previous results [8] **for optimal design sizing for 60-days replenishment (Isp = 2600 s, Thrust =1.025 N, Power = 20 kW)**

Parameters	MISS Results	MAGNETO (MISS v2) Results	Percentage
Propellant Mass GTO-NRHO [kg]	1976	1132	-43%
Propellant Mass NRHO-GTO [kg]	1255	695	-45%
LST Dry Mass [kg]	5240.6	6264 (*)	+16%
LST Wet Mass [kg]	15622.24	13635	-13%
Transfer Time GTO-NRHO [days]	488.70	382	-22%
(*) Different assumption on EPS, TCS and AOCS			

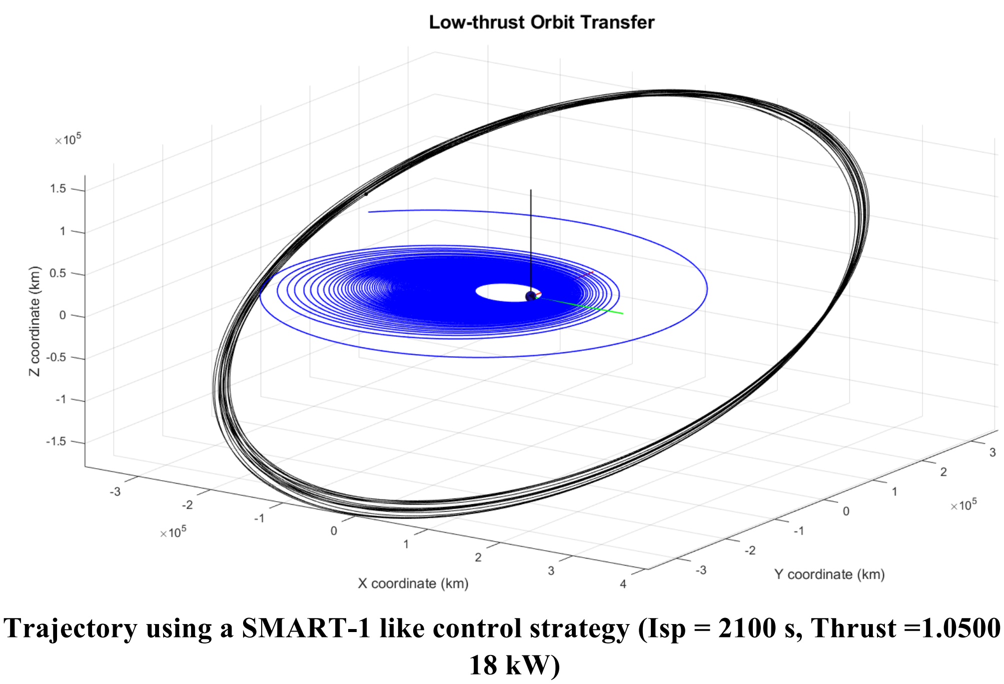

Figure 4: Trajectory using a SMART-1 like control strategy (Isp = 2100 s, Thrust =1.0500 N, Power = 18 kW)

5. CONCLUSIONS AND FUTURE WORK

In this paper, the architecture and the potentiality of the electric propulsion platform sizing tool MAGNETO are presented. The tool may be used to simulate near-Earth scenarios as well as Cislunar scenario. It performs a series of iterations of different LST configurations in terms of cargo mass, thruster numbers and characteristics until convergence on the overall launch mass is reached. The user may analyse the impact on delta-V, transfer time and propellant mass of diverse thrusting laws and propulsion system and payload general characteristics. Eventually, the outputs of MAGNETO provide a design envelope to study of cargo transportation systems for space applications.

If we compare MAGNETO with MISS, it is clear that the build-in trajectory, in the simulation loop, improves the estimation of the overall wet mass decreasing it of 10% in respect of the MISS value. The results show a reduction of the overall propellant mass around 40% and a transfer time diminished by 20%. The consumed propellant mass, evaluated throughout the trajectory, shows almost no deviation from the GMAT output.

Ultimately, a reliable tool that can evaluate different configuration of the space tug has been created. The tool is flexible and defines the design envelope for the study of space cargo systems propelled with electric propulsion.

The PoliTO team is now focusing on extending the tool towards Low Mars Orbit (LMO) and beyond. This will enrich the reference mission choices and the design space of the MAGNETO software. Furthermore, the work on the trajectory will focus on a more accurate modelling of the drag and solar pressure perturbations. Likewise, work is undergoing in order to refine the design of the main subsystems as well as to improve the sizing for CDH, TT&C and Structure and Mechanism is now under development. Currently, the PoliTO team is thinking of extending the tool toward the satisfaction of other objectives such as the maximization of the cargo module and the minimization of time. However, this will be a following step after the subsystem analysis refinement.

REFERENCES

[1] I. S. E. C. Group, "The Global Exploration Roadmap," Tech. report , 2018.

[2] S. Cresto Aleina, N. Viola, F. Stesina, M. A. Viscio and S. Ferraris, "Reusable space tug concept and mission," *Acta Astronautica,* vol. 128, pp. 21-32, 2016.

[3] G. Genta and P. Maffione, "Optimal low-thrust trajectories for nuclear and solar electric propulsion," *Acta Astronautica,* vol. 118, pp. 251-261, 2016.

[4] L. Casalino, G. Colasurdo and M. Sentinella, "Indirect optimization Method for Low-Thrust Interplanetary Trajectories," in *30th International Electric Propulsion Conference*, Florence, 2007.

[5] J. T. Howell, M. J. O'Neill and J. C. Mankins, "High-voltage array ground test for direct-drive solar electric propulsion," *Acta Astronautica,* vol. 59, pp. 206-215, 2006.

[6] J. Wertz and W. Larson, Space Mission Analysis and Design, El Segundo: Microcosm Press and Kluwer Academic Publishers, 1999.

[7] M. Mammarella, C. Paissoni, N. Viola, A. Denaro, E. Gargioli and F. Massobrio, "The Lunar Space Tug: A sustainable bridge between low Earth Orbits and Cislunar Habitat," *Acta Astronautica,* vol. 138, pp. 102-117, 2017.

[8] M. Mammarella, *A Comprehensive Modeling Framework for Integrated Mission Analysis and Design of a Reusable Electric Space Tug,* Torino: Politecnico di Torino, 2018.

[9] M. Mammarella, P. M. Vernicari, C. A. Paissoni and N. Viola, "How the Lunar Space Tug can support the cislunar station," *Acta Astronautica,* vol. 154, pp. 181-194, 2019.

[10] A. Space, "Ariane 6 User's Manual," Ariane Group, 2018.

[11] C. A. Paissoni, J. Rimani, N. Viola and T. Andreussi, "GEO telecomunication satellite: new opportunities enabled by 20kW class Hall thrusters," in *70th International Astronautical Congress*, Washington, 2019.

[12] J. Schoenmaekers, "Post-launch Optimisation of the SMART-1 Low-thrust Trajectory to the Moon," in *Proceedings of the 18th International Symposium on Space Flight Dynamics (ESA SP-548)*, Munich, Germany, 2004.

[13] R. Biesbroek, Lunar and Interplanetary Trajectories, AG Switzerland: Springer International Publishing Switzerland, 2016.

[14] ESA, "Margin Philosophy for Science Assessment Studies - Issue 1 Revision 3," 2012.

[15] H. Curtis, Orbital Mechanics for Engineering Students, Oxford: Elsevier, 2005.

[16] C. Rampersad, "Preliminary Design of a Very-Low-Thrust Geostationary Transfer Orbit to Sun-Synchronous Orbit Small Satellite Transfer," University of Toronto, Toronto, 2004.

[17] Springer, "Dynamic Models Of Satellite Relative Motion Around an Oblate Earth," [Online]. Available: http://www.springer.com/978-981-10-2382-8 . [Accessed 1 2019].

[18] R. H. Battin, An Introduction to the Mathematics and Methods of Astrodynamics, Reston: AIAA, 1999.

[19] D. A. Vallado, Fundamentals of Astrodynamics and Applications, Springer Netherlands, 2001.

[20] J. T. Betts, "Optimal low–thrust orbit transfers with eclipsing," *Applied Mathematical Analysis,* vol. 36, no. 2, pp. 218-240, 2014.

[21] A. Ruggiero, P. Pergola, S. Marcuccio and M. Andrenucci, "Low-Thrust Maneuvers for the Efficient Correction of Orbital Elements.," in *32th International Electric Propulsion Conference*, Wiesbaden, 2011.

[22] C. R. Ortiz Longo and S. L. Rickman, "Method for the Calculation of Spacecraft Umbra and Penumbra Shadow Terminator Points," NASA Technical Paper 3547, Houston, Texas, 1995.

[23] "The SPICE Toolkit," Jet Propulsion Laboratory, 10 April 2017. [Online]. Available: https://naif.jpl.nasa.gov/naif/toolkit.html. [Accessed 17 November 2019].